Original Article

The prognostic and immune significance of *SNHG3* in clear cell renal cell carcinoma

Cheng Li[#], Pengnan Hu[#], Chenglong Fan[#], Hua Mi

Department of Urology, The First Affiliated Hospital of Guangxi Medical University, Nanning, China

Contributions: (I) Conception and design: C Li, P Hu; (II) Administrative support: H Mi; (III) Provision of study materials or patients: P Hu; (IV) Collection and assembly of data: C Fan; (V) Data analysis and interpretation: All authors; (VI) Manuscript writing: All authors; (VII) Final approval of manuscript: All authors.

[#]These authors contributed equally to this work.

Correspondence to: Hua Mi, PhD. Department of Urology, The First Affiliated Hospital of Guangxi Medical University, No. 6 Shuangyong Street, Nanning 530021, China. Email: mihua2019@163.com.

Background: Long non-coding RNA (lncRNA) small nucleolar RNA host gene 3 (*SNHG3*) has been reported to be involved in the pathological process of a variety of tumors, including clear cell renal cell carcinoma (ccRCC). However, whether *SNHG3* can be used as a prognostic biomarker and its correlation with immune infiltration in ccRCC remain unclear, warranting further research. This study aims to explore the relationship between *SNHG3* and immune infiltration in ccRCC and confirm the potential of *SNHG3* to predict survival of ccRCC patients.

Methods: The Cancer Genome Atlas (TCGA) database was used to assess the expression of *SNHG3* in ccRCC, evaluate clinicopathological characteristics, assess prognosis, and conduct functional enrichment analysis. The ccRCC microenvironment and immune infiltration were investigated using the Estimation of STromal and Immune cells in MAlignant Tumor tissues using Expression data (ESTIMATE) and Cell-type Identification By Estimating Relative Subsets Of RNA Transcripts (CIBERSORT) algorithms, respectively. We additionally investigated the relationships between *SNHG3* and immunological checkpoints. Drug sensitivity of *SNHG3* was investigated in R. The expression of *SNHG3* was verified in the Gene Expression Omnibus (GEO) database, ccRCC cell lines, and tissues. Wound healing and Methylthiazolyldiphenyl-tetrazolium bromide (MTT) assays were used to evaluate tumor cell migration and proliferation. Fluorescence in situ hybridization (FISH) assay was conducted to localize *SNHG3* in ccRCC cells.

Results: *SNHG3* expression was significantly upregulated in ccRCC cells and tissues and associated with several clinicopathological features and poor prognosis of ccRCC patients. *SNHG3* was correlated with immune cells infiltration in ccRCC and exhibited sensitivity to various targeted and chemotherapy drugs. Knockdown of *SNHG3* significantly reduced the proliferation and migration of ccRCC. FISH results showed that *SNHG3* was located in the cell nucleus.

Conclusions: Overall, this study demonstrates that *SNHG3* is a prognostic biomarker correlated with immune infiltration in ccRCC.

Keywords: *SNHG3*; immune infiltration; prognosis; drug sensitivity; clear cell renal cell carcinoma (ccRCC)

Submitted Aug 25, 2024. Accepted for publication Dec 17, 2024. Published online Feb 26, 2025.
doi: 10.21037/tcr-24-1509
View this article at: https://dx.doi.org/10.21037/tcr-24-1509

Introduction

One of the most common types of kidney cancer and the second leading cause of urologic malignancy-related mortality is renal cell carcinoma (RCC). As of 2024, there were approximately 81,610 new cases of RCC in the United States, with an annual incidence rate of 1.5 percent (1). There are approximately 75% cases of clear cell renal cell carcinoma (ccRCC), which is RCC's most prevalent subtype (2). Because ccRCC is not sensitive to conventional radiotherapy and chemotherapy, surgery remains the most effective treatment method (3). However, 10% to 30% of individuals with ccRCC eventually experience metastases after surgery (4). Finding novel biomarkers that link to the immunological microenvironment of ccRCC and regulate its prognosis is therefore urgently needed.

The majority of human genomic DNA is transcribed into non-coding RNA instead of messenger RNA (mRNA) (5). An RNA sequence with no more than 200 nucleotides that does not encode a polypeptide or protein is called a long non-coding RNA (lncRNA) (6). It has been proven that lncRNAs can regulate tumor development, such as *LINC01535*, which promotes the proliferation capacity and migration level of breast cancer via regulating *miR-214-3p* (7). In addition, some lncRNAs have been associated with tumor immune cell infiltration. For example, the level of *LINC00963* in cervical cancer was associated with immune cell infiltration and poor survival according to Chang *et al.* (8). Peng *et al.* demonstrated that high expression of lncRNA myocardial infarction associated transcript (*MIAT*) mediates immune escape by upregulating programmed death-ligand 1 (PD-L1) in hepatocellular carcinoma (9). The above studies overlap in their assertion of the huge potential of lncRNAs to regulate tumor progression, providing the possibility for combining targeted therapy and immunotherapy.

As described in the reported literatures, lncRNA small nucleolar RNA host gene 3 (*SNHG3*) regulates various tumors, including ccRCC, among the numerous lncRNAs. It has been established that *SNHG3* regulates NEIL3 to mediate the poor outcomes of hepatocellular carcinoma patients (10). Xu *et al.* demonstrated that *SNHG3* promotes the progression of ccRCC via regulating BIRC5 expression (11). Moreover, *SNHG3* has been associated with immune infiltration in non-neoplastic diseases. Huang *et al.* identified *SNHG3* as one of the key genes regulating immunity in children with Henoch Schönlein purpura nephritis (12). *SNHG3-miR-139-5p*-TOP2A has been reported to link to the prognosis of ccRCC by pan-cancer analysis of RNA sequencing data. Meanwhile, TOP2A reportedly has the function of regulating immune cells (13). Despite these findings illustrating the regulatory involvement of *SNHG3* in tumors and immune interactions, whether *SNHG3* is related to immune infiltration in ccRCC remains unclear.

This study aims to explore the relationship between *SNHG3* and immune infiltration in ccRCC and confirm the potential of *SNHG3* to predict survival of ccRCC patients. The analytical workflow of the research is described in *Figure 1*. Meanwhile, we propose speculation that *SNHG3* and immune infiltration are related through bioinformatics analysis and experimental validation, thus offering a new target for the clinical treatment of ccRCC. We present this article in accordance with the MDAR reporting checklist (available at https://tcr.amegroups.com/article/view/10.21037/tcr-24-1509/rc).

Highlight box

Key findings

- Small nucleolar RNA host gene 3 (*SNHG3*) could be a potential marker for predicting prognosis of clear cell renal cell carcinoma (ccRCC).

What is known and what is new?

- *SNHG3* promotes the proliferation and migration of ccRCC cells.
- *SNHG3* is associated with immune cell infiltration in ccRCC. These study findings offer insights for a better understanding of the prevention and treatment of ccRCC and provide the foundation for precision medicine.

What is the implication, and what should change now?

- The immune infiltration relationship between *SNHG3* and ccRCC and whether *SNHG3* can be used as a prognostic biomarker for ccRCC are still unclear. Future studies should be conducted using more datasets to validate the current findings, thus establishing the prognosis model based on clinical data and *SNHG3*.

Methods

Bioinformatics analysis

A dataset consisting of gene expression profiles from 72 normal tissues and 541 tumor tissues of ccRCC was downloaded from The Cancer Genome Atlas (TCGA) database (https://www.cancer.gov/ccg/research/genome-sequencing/tcga). The normal tissues were considered as the control group. Differentially expression analysis was performed using the R package "limma", with criteria for identifying differentially expressed genes (DEGs) set as |log fold change (FC)| >1.5 and false discovery rate (FDR) <0.05 (14).

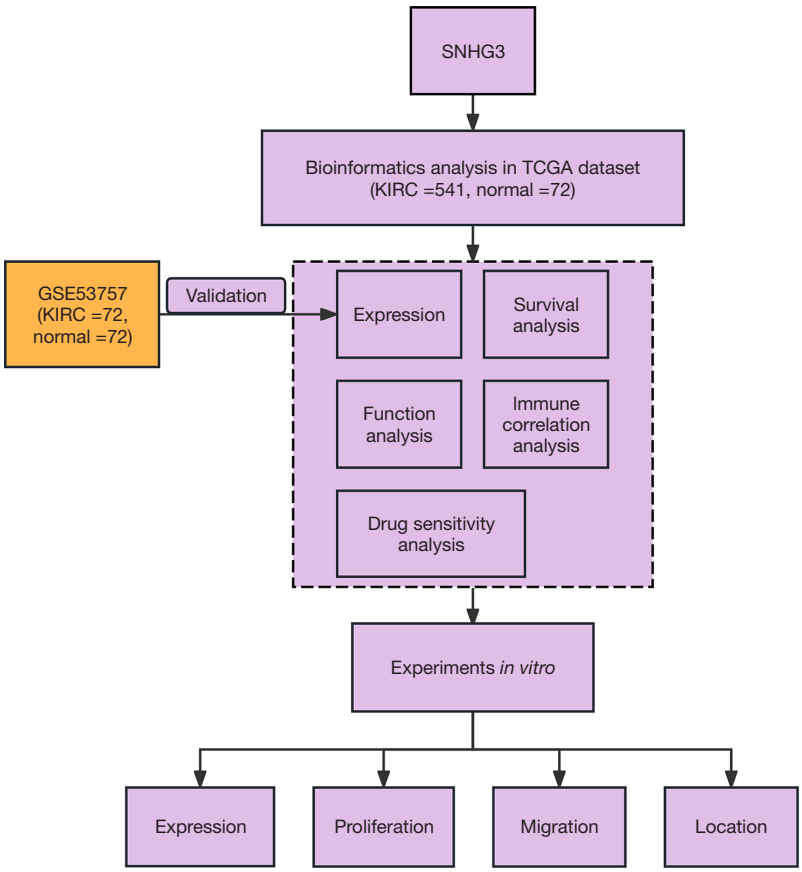

Figure 1 Analytical workflow of *SNHG3*. TCGA, The Cancer Genome Atlas; KIRC, Kidney Renal Clear Cell Carcinoma.

Survival analysis was conducted using the R package "survival" to investigate the correlation between *SNHG3* and the prognosis of ccRCC patients (15). To validate the findings, the original gene expression profile (GSE53757) was obtained from the Gene Expression Omnibus (GEO) database (https://www.ncbi.nlm.nih.gov/geo/).

Gene Ontology (GO) enrichment analysis and Kyoto Encyclopedia of Genes and Genomes (KEGG) pathway analysis were carried out using "clusterProfiler" package (16). Gene Set Enrichment Analysis (GSEA) was utilized to evaluate metabolic pathways and biological functions.

Immune cell infiltration analysis

Immune cell infiltration analysis was conducted using the Estimation of STromal and Immune cells in MAlignant Tumor tissues using Expression data (ESTIMATE) algorithm (17). This allowed calculation of immune scores, stromal scores, and estimate scores for each sample from TCGA. The correlation between *SNHG3* and immune cells was assessed, and the Cell-type Identification By Estimating Relative Subsets Of RNA Transcripts (CIBERSORT) algorithm was employed to determine differences in immune cell infiltration between high and low *SNHG3* expression groups (18). Furthermore, using TIMER2.0 (http://timer.cistrome.org/), a survival analysis of *SNHG3* and *SNHG3*-expressing immune cells in ccRCC was performed. The relationship between *SNHG3* expression and immune checkpoints was also explored (19).

Immunotherapy and drug sensitivity analysis

The effect of immunotherapy on *SNHG3* was studied based on The Cancer Immunome Atlas (TCIA) (https://www.tcia.at/) database (20). The effect of chemotherapeutics and targeted agents on *SNHG3* was studied using the Computational Analysis of Resistance (CARE) (http://care.dfci.harvard.edu/) database (21). Subsequently, the "pRRophetic" package was used in R to study the drug sensitivity differences between the high *SNHG3* expression

group and the low *SNHG3* expression group (22). The drug sensitivity was predicted by calculating the half-maximal inhibitory concentration (IC_{50}) of chemotherapy and targeted agents.

Cell culture

The human renal cancer cell line 786-O (WHELAB C1043) and immortalized renal tubular epithelial cell HK-2 (WHELAB C116) were provided by SHANGHAI WHELAB BIOCIENCE LIMITED. Cell lines were authenticated by the supplier. 786-O and HK-2 were cultivated in Dulbecco's Modified Eagle Medium (DMEM) complete medium in a humidified atmosphere of 5% CO_2 at 37 ℃.

Clinical samples

Clinical samples including ccRCC tissues and adjacent normal tissues (n=8) were acquired from the same patients who underwent radical nephrectomy at the First Affiliated Hospital of Guangxi Medical University and rapidly stored in liquid nitrogen for further experiments. Corresponding adjacent noncancerous tissues were obtained from sites at least 5 cm away from the cancerous region. The study was conducted in accordance with the Declaration of Helsinki (as revised in 2013). The study was approved by the Ethics Review Committee of the First Affiliated Hospital of Guangxi Medical University (approval No. 2023-E302-01) and informed consent was taken from all individual participants.

Quantitative reverse transcription-polymerase chain reaction (qRT-PCR)

To examine *SNHG3* expression in ccRCC cell lines and tissues, we performed qRT-PCR analysis. Total RNA was extracted with TRIzol (Invitrogen, USA) according to the manufacturer's protocol. The primer sequences were obtained from Sangon Biotech (Shanghai, China) as follows: *SNHG3*: Forward 5'-AGTGGTCGCTTCTTCTCCTTG-3', Reverse: 5'-GATTGTCAAACCCTCCCTGTTA-3'. *β-actin*: Forward 5'-GTCATTCCAAATATGAGATGCGT-3', reverse 5'-GCTATCACCTCCCCTGTGTG-3'. Relative expression levels were calculated according to the 2-ΔΔCt method. Statistical analyses were performed with GraphPad Prism.

Cell transfection

Small interfering RNAs (siRNAs) specifically targeting *SNHG3* and their negative control (si-*NC*) were synthesized by Sangon (Shanghai, China). The primer sequences were as follows, si-*SNHG3*-1: Forward 5'-GCUAGGAAUGCACAUUCUUTT-3', reverse 5'-AAGAAUGUGCAUUCCUAGCTT-3'. Si-*SNHG3*-2: Forward 5'-CCUAGCUGAUGAGUUGUAUTT-3', reverse 5'-AUACAACUCAUCAGCUAGGTT-3'. Si-*NC*: Forward 5'-UUCUCCGAACGUGUCACGUTT-3', reverse 5'-ACGUGACACGUUCGGAGAATT-3'. A total of 10 pmol of siRNA was transfected into 786-O cells using liposome RNAiMAX (Invitrogen, USA) in each group separately. After 48 h of transfection, the transfection efficiency was measured by qRT-PCR, and the cells were collected for subsequent experiments.

Wound healing assay

A total of 50×10^4 cells were seeded in 6-well plates and incubated in a constant temperature incubator at 37 ℃ and 5% CO_2 for 12 h. The migration of cells was observed and recorded by light microscopy and photography We analyzed five image fields for the control group and four image fields for each of the two treatment groups and the blank area was measured by Image J software. Relative migration rate was calculated by normalizing the distance of the blank area at 0 h.

Methylthiazolyldiphenyl-tetrazolium bromide (MTT)

First, 100 μL of medium containing 4–5 $\times10^3$ ccRCC cells was seeded in each well of a 96-well plate. After 0, 24, 48, and 72 h, 20 μL of MTT solution was introduced into each well and incubated for 4 h at 37 ℃ and 5% carbon dioxide. Then, 150 μL of dimethyl sulfoxide (DMSO) was added to the discarded solution and shaken. The optical density (OD) at 490 nm wavelength was measured. Each experimental group at each time point was performed with at least three independent replicates (n≥3) to ensure the reliability of the results.

Fluorescence in situ hybridization (FISH)

To examine the localization of *SNHG3* in HK-2 and 786-O cells, FISH experiments were performed by Servicebio (Wuhan, China). *SNHG3* probes were synthesized by Servicebio. HK-2 and 786-O cells were cultured on glass slides and fixed with *in situ* hybridization fixative for

20 minutes at room temperature. Protease K (20 μg/mL) was then applied to the slides for digestion at 37 ℃. A pre-hybridization solution was added dropwise and incubated at 37 ℃ for 1 hour. After discarding the pre-hybridization solution, a probe-containing hybridization solution was added, and slides were incubated overnight. Following hybridization, slides were washed sequentially with 2 × saline sodium citrate (SSC) buffer at 37 ℃ for 10 minutes, 1 × SSC at 37 ℃ for 2 intervals of 5 minutes each, and 0.5 × SSC at room temperature for 10 minutes. A preheated branch-specific probe hybridization solution (60 μL) was then added dropwise, and the slides were incubated in a humidified chamber at 40 ℃ for 45 minutes. Post-hybridization washes were repeated as above. Nuclei were counterstained with 4', 6-diamidino-2-phenylindole (DAPI) for 8 minutes. Images were captured under a Nikon upright fluorescence microscope (Japan) using a 20× objective.

Statistical analysis

Statistical analyses were conducted using SPSS 22.0 and GraphPad Prism 8.0.2. Student's *t*-test, one-way ANOVA, and rank sum test were employed for comparing parametric and non-parametric data. Univariate and multivariate Cox regression analyses were performed to analyze *SNHG3*-related clinicopathological features. Pearson's correlation coefficient was used to assess the linear relationship, and survival analysis was conducted using the log-rank test. Each experiment was performed at least three times to ensure reproducibility. Statistical significance was determined at P<0.05.

Results

The expression of SNHG3 is upregulated in ccRCC

The RNA-sequence data of 72 normal tissues and 541 ccRCC tissues were extracted from TCGA. In ccRCC tissues, *SNHG3* expression was higher than in normal tissues (P<0.001; *Figure 2A*). To validate this finding, we then extracted the data of 72 pairs of ccRCC tissues from a GEO dataset (GSE53757) to perform analysis (23). Consistently, we observed a similar upregulation of *SNHG3* expression in ccRCC (P<0.001; *Figure 2B*).

Upregulation of SNHG3 expression predicts poor prognosis in ccRCC patients

To verify whether *SNHG3* could play a role as an independent prognostic factor for ccRCC, the relationship between *SNHG3* expression level and clinicopathological parameters (histologic grade, T stage, distant metastasis, and lymph node infiltration) in ccRCC was evaluated. The analysis results of TCGA-Kidney renal clear cell carcinoma (KIRC) illustrated that *SNHG3* expression differences were observed between grade 2 and grade 4 (P=0.002; *Figure 2C*), and grade 3 and grade 4 (P=0.02; *Figure 2C*). *SNHG3* expression showed significant differences between T1 and T3 (P=0.009; *Figure 2D*), T4 (P<0.001; *Figure 2D*), T2 and T4 (P<0.001; *Figure 2D*), and T3 and T4 (P=0.007; *Figure 2D*). Additionally, *SNHG3* expression exhibited significant differences in cases of not only distant metastasis but also lymph node infiltration in ccRCC (P<0.001, *Figure 2E*; P=0.008, *Figure 2F*). Furthermore, univariate and multivariate Cox regression analyses were performed. Univariate Cox regression analysis showed that *SNHG3*, age, grade, and stage were associated with ccRCC prognosis (P<0.001; *Figure 2G*); multivariate Cox regression analysis, which included the above factors with P values less than 0.05, showed that *SNHG3*, age, grade, and stage were associated with ccRCC prognosis and hazard ratio (HR) >1 (P<0.001; *Figure 2H*). The results suggested that elevated *SNHG3* expression predicted poor outcomes as an independent prognostic biomarker in ccRCC.

To verify whether elevated *SNHG3* expression had an impact on ccRCC patient survival, we extracted the survival data from TCGA-KIRC. To better understand whether there is an association and difference between *SNHG3* expression levels and survival of ccRCC patients, the patients were categorized based on median *SNHG3* expression into low and high *SNHG3* expression groups and survival analyses were conducted. Based on Kaplan-Meier curves, the higher *SNHG3* expression group had significantly lower overall survival (OS) than the low expression group (P<0.001; *Figure 2I*). High *SNHG3* expression was associated with a lower progression-free survival (PFS) than low expression (P=0.006; *Figure 2J*). Finally, receiver operating characteristic (ROC) curve analysis showed that *SNHG3* had the ability to predict the future prognosis of ccRCC patients. The areas under the curve (AUCs) at 1, 3, and 5 years were 0.665, 0.651, and 0.693, respectively (*Figure 2K*).

Functional enrichment analysis reveals that SNHG3 is related to cellular life activities

CcRCC patients' gene expression profile was extracted

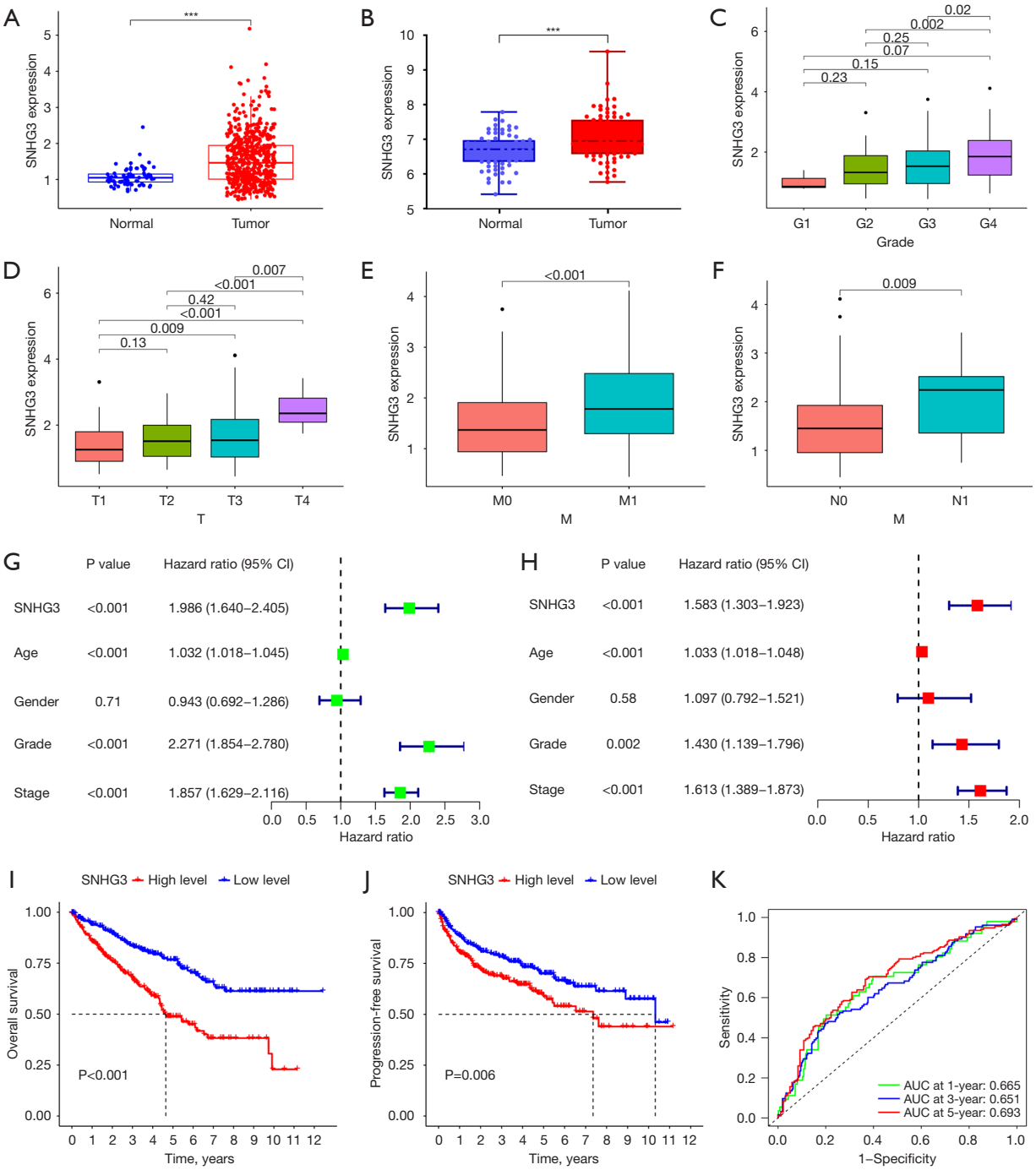

Figure 2 *SNHG3* is upregulated and associated with various clinicopathological parameters in ccRCC. (A) The expression of *SNHG3* in 541 ccRCC tissues and 72 normal tissues based on data from TCGA database. (B) The expression level of *SNHG3* based on data from the GEO dataset (GSE53757) (n=72). (C-F) Differences in *SNHG3* expression level with different clinicopathological features: histologic grade, T stage (T), distant metastasis (M), and lymph node infiltration (N) in ccRCC. (G) Univariate Cox regression analysis. (H) Multivariate Cox regression analysis. (I,J) The Kaplan-Meier curves of *SNHG3* in ccRCC for both overall survival and progression-free survival. (K) The AUCs at 1-, 3-, and 5-year for *SNHG3*. ***, P<0.001. ccRCC, clear cell renal cell carcinoma; TCGA, The Cancer Genome Atlas; GEO, Gene Expression Omnibus; CI, confidence interval; AUCs, areas under the curve.

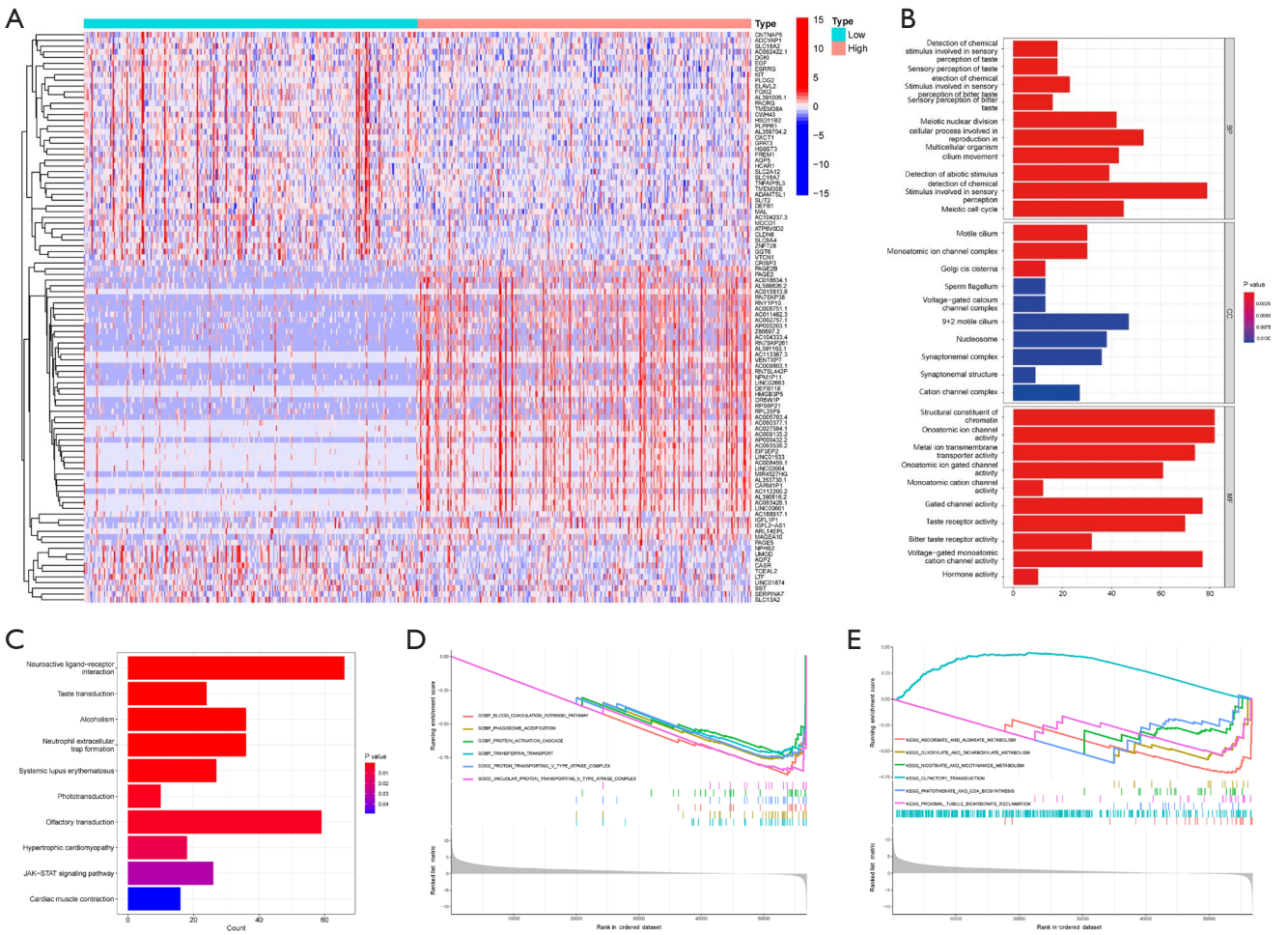

Figure 3 Enrichment analyses of differentially expressed DEGs. (A) Heatmap of DEGs. CcRCC patients were divided into high- and low-expression groups based on the median expression value of *SNHG3*. (B) GO analysis. (C) KEGG analysis. (D) Six biological functions related to *SNHG3* by GSEA analysis. (E) Six metabolic pathways related to *SNHG3* by GSEA analysis. DEG, differentially expressed genes; ccRCC, clear cell renal cell carcinoma; GO, Gene Ontology; BP, biological process; CC, cellular component; MF, molecular function; KEGG, Kyoto Encyclopedia of Genes and Genomes; GSEA, Gene Set Enrichment Analysis.

from TCGA-KIRC. Based on the median expression value of *SNHG3*, ccRCC patients were divided into high- and low-expression groups, and 117 DEGs in both groups were visualized in heatmaps, including 93 upregulated genes and 24 downregulated genes (*Figure 3A*).

To explore the potential functions of those DEGs, GO and KEGG analyses were performed in this study. GO annotation showed significant enrichment of DEGs in multiple cellular life activity-related pathways, such as meiotic nuclear division, cilium movement, DNA packaging complex and protein-DNA complex, etc., suggesting that *SNHG3* may involve in cell proliferation and division (*Figure 3B*). KEGG analysis showed significant enrichment of DEGs in neuroactive ligand–receptor interaction, taste transduction, alcoholism, neutrophil extracellular trap formation pathway, etc (*Figure 3C*).

To find out the role *SNHG3* played in ccRCC, GSEA was conducted to explore the biological functions and metabolic pathways connected with *SNHG3*. Specifically, *SNHG3* was found to be related to blood coagulation intrinsic pathway, phagosome acidification, protein activation cascade, transferrin transport, proton transporting V-type ATPase complex, and vascular proton transporting V-type ATPase complex (*Figure 3D*). Additionally, *SNHG3* was associated with metabolic pathways such as ascorbate and aldarate metabolism, glyoxylate and dicarboxylate

metabolism, nicotinate, and nicotinamide metabolism, olfactory transduction, pantothenate and CoA biosynthesis, and proximal tubule bicarbonate reclamation (*Figure 3E*). These findings indicate that *SNHG3* is involved in various cellular life activities.

SNHG3 plays a role in the immune microenvironment of ccRCC

After grouping by *SNHG3* expression median values, the *SNHG3* high expression group had significantly higher immune scores than the *SNHG3* low expression group by using the ESTIMATE algorithm (P<0.001), while the stromal score showed no differences between the two groups (*Figure 4A*), which suggested that *SNHG3* expression was connected with immune cell infiltration in the ccRCC microenvironment to some extent.

Further, we evaluated the relationship between *SNHG3* expression and each immune cell in ccRCC, among which follicular helper T cells, T cells regulatory (Tregs), memory B cells, and activated CD4 T memory cells were positively correlated with *SNHG3*, while M2 macrophages, resting CD4 T memory cells, activated dendritic cells, resting mast cells were negatively correlated with *SNHG3* (*Figure 4B*). The relationship between *SNHG3* and each immune cell type was shown separately by linear plots (*Figure 4C-4J*).

Subsequently, by using the CIBERSORT algorithm, we explored the ability of *SNHG3* to influence the distribution of immune infiltrating cells in ccRCC. After grouping, the results showed that follicular helper T cells, Tregs, and activated dendritic cells were abundant in the *SNHG3* high expression group; naive B cells, M0 macrophages, and resting mast cells were more abundant in the *SNHG3* low expression group (*Figure 4K*).

Since *SNHG3* demonstrated an association with the above immune cells, we would like to find out whether the survival of ccRCC patients changes under different states of immune cell infiltration. So we performed survival analyses based on TIMER2.0, combined with different immune infiltrated cells in *Figure 4K*. We discovered that elevated levels of M0 macrophages, Tregs, and follicular helper T cells led to a poorer prognosis in ccRCC patients in the *SNHG3* high expression group (P<0.05); however, in the *SNHG3* low expression group, M0 macrophage, Tregs, and follicular helper T cells levels had no significant differences on the prognosis (P>0.05; *Figure 4L-4N*). These results further suggested that *SNHG3* was associated with various immune cells.

SNHG3 is sensitive to immunotherapy, chemotherapy, and targeted drugs

The upregulation of immunosuppressive checkpoints by tumor cells is one of the factors that contribute to immune escape, which is now known to be one of the mechanisms that promote tumor progression. We evaluated the relationships between the expression of *SNHG3* and several immunological checkpoints (*Figure 4O*). The findings demonstrated a favorable correlation between *SNHG3* expression in ccRCC and a number of inhibitory checkpoint molecules, including TNFSF14, IDO2, TNFRSF25, CTLA4 and TNFRSF18. All relevant immunosuppressive

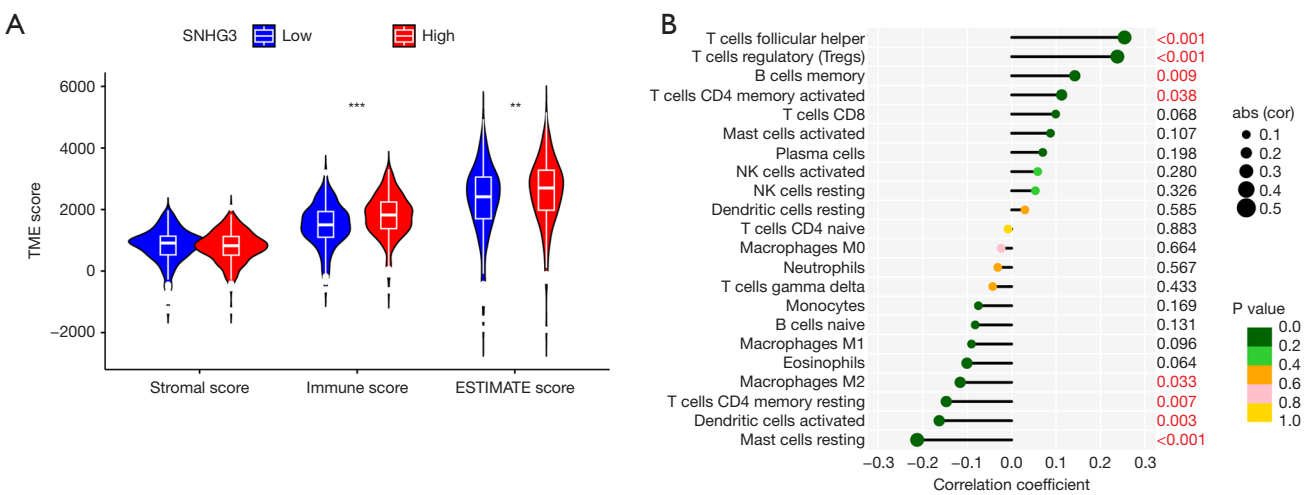

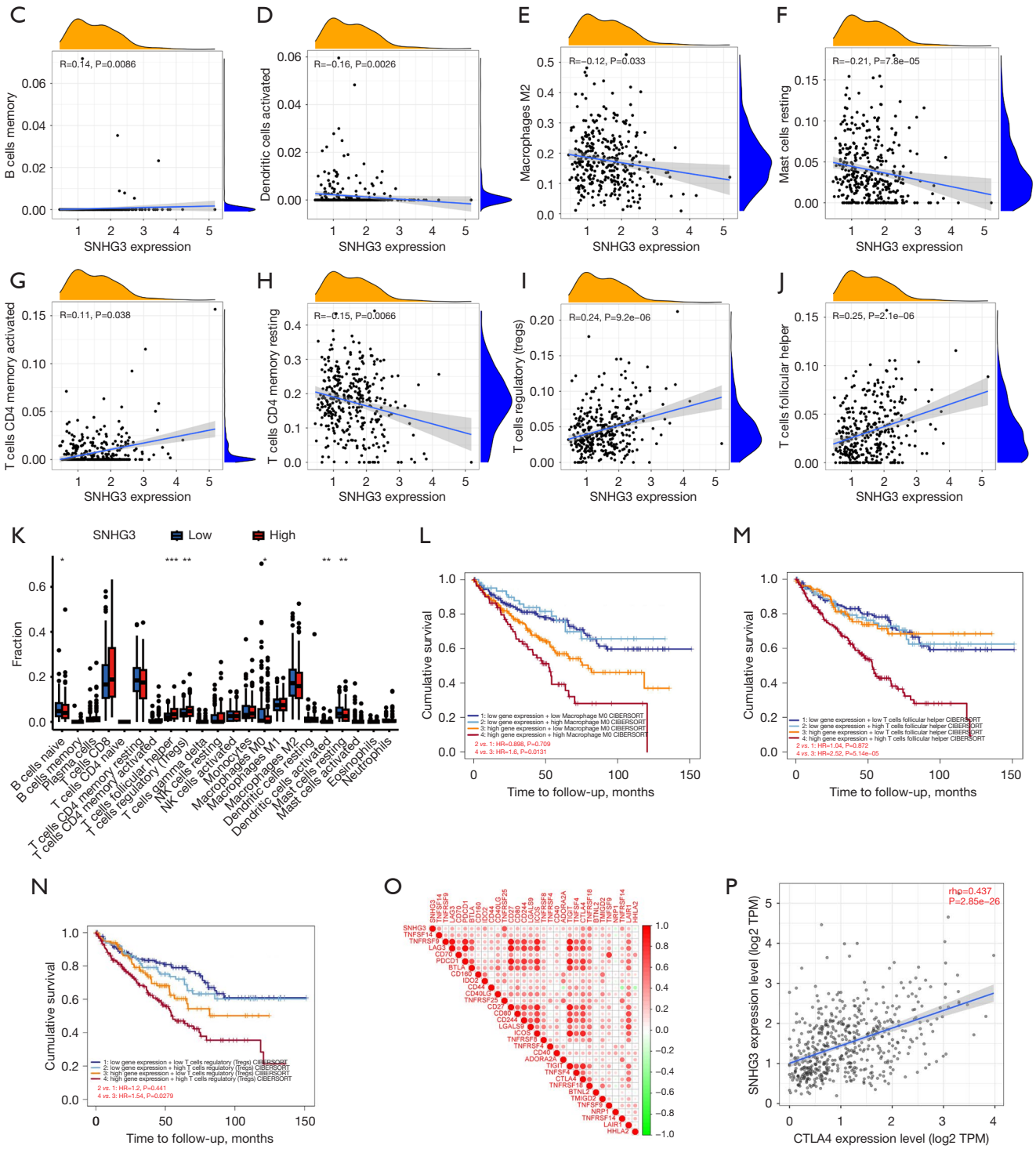

Figure 4 Tumor immune microenvironment analysis. (A) Immune score and stromal score in the *SNHG3* high expression group and low expression group. (B) *SNHG3*-associated immune cells. (C-J) Display of *SNHG3*-related immune cells, separately. (K) Immune cell infiltration in the *SNHG3* high expression group and low expression group. (L-N) Effect of *SNHG3* expression and immune cells infiltration on the prognosis of ccRCC patients. (O) Correlation between *SNHG3* and immune checkpoints. (P) CTLA4 was positively correlated with *SNHG3* expression. *, P<0.05; **, P<0.005; ***, P<0.001. TME, tumor microenvironment; ccRCC, clear cell renal cell carcinoma; HR, hazard ratio; TPM, transcripts per million.

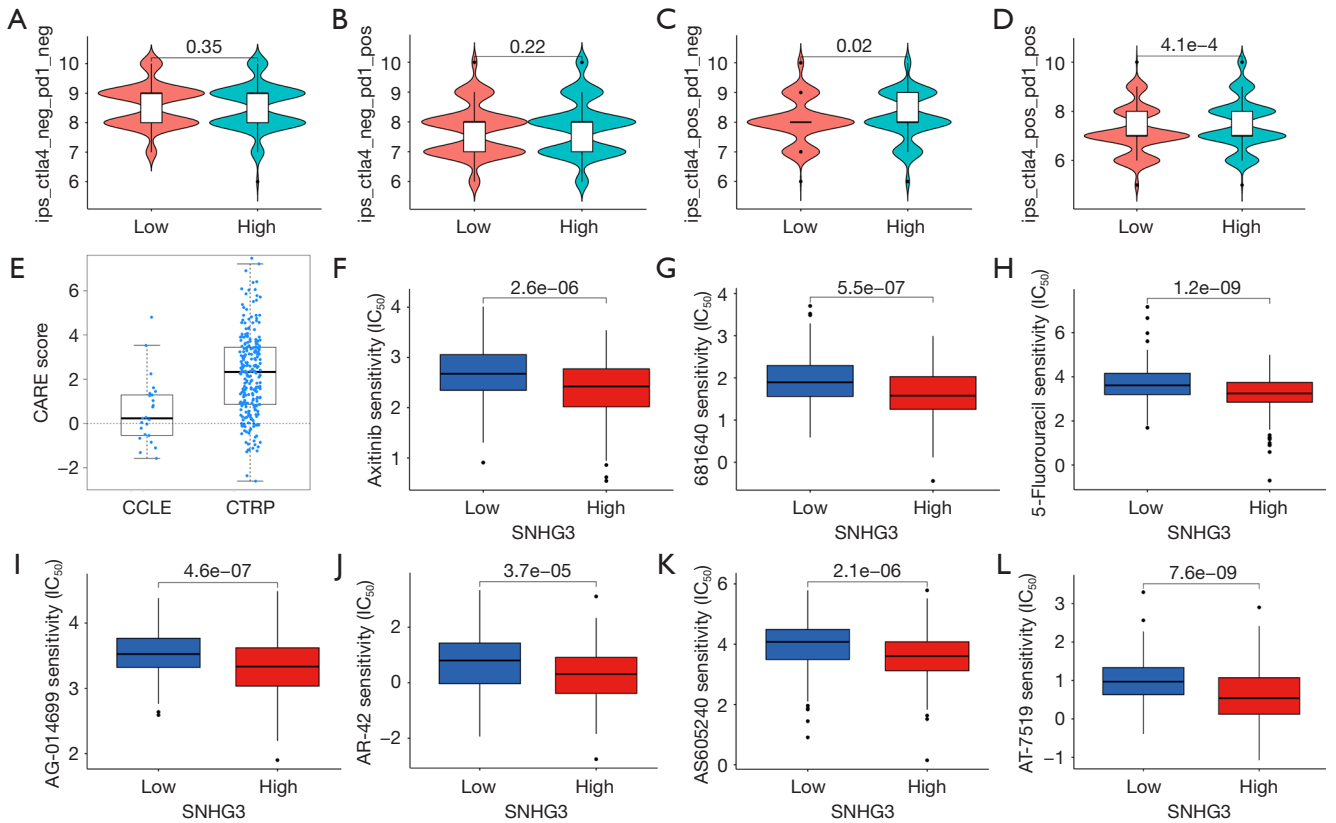

Figure 5 Immunotherapy and drug sensitivity analysis. (A-D) Differential analysis of immune treatment in the high and low *SNHG3* expression groups. (E) The CARE scores indicated that most chemotherapeutics and targeted drugs of the CCLE and the CTRP were effective against *SNHG3*. (F-L) Drug sensitivity analysis. CARE, Computational Analysis of Resistance; CCLE, Cancer Cell Line Encyclopedia; CTRP, Cancer Therapeutics Response Portal; IC_{50}, half-maximal inhibitory concentration.

checkpoints were performed correlation analysis in TIMER2.0. Only CTLA4 was positively correlated with *SNHG3* expression, suggesting a close relationship between *SNHG3* expression and CTLA4 expression (*Figure 4P*). We also explored the variations in sensitivity to immunotherapies, chemotherapy, and targeted medications between the *SNHG3* high- and low-expression groups in order to enhance the outcomes of ccRCC patients. With a mean score of 8.0645 for the *SNHG3* low expression group and 8.21875 for the *SNHG3* high expression group, the analysis of immunotherapies based on TCIA revealed that anti-CTLA4 treatment was effective in the *SNHG3* high expression group (*Figure 5A-5D*). Based on CARE scores, we found that most drugs in the Cancer Cell Line Encyclopedia (CCLE) and the Cancer Therapeutics Response Portal (CTRP) were effective against *SNHG3* (*Figure 5E*). The IC_{50} of axitinib, 681640, 5-fluorouracil, AG-014699, AR-42, AS605240, and AT-7519 were later discovered to be greater in patients in the *SNHG3* low expression group than in the high expression group using the R package "pRophetic" (*Figure 5F-5L*). The *SNHG3* high-expression group may be more susceptible to these medications, we concluded.

Effects of SNHG3 on expression, proliferation, and migration of ccRCC cells, and SNHG3 is distributed in the cell nucleus

To confirm that *SNHG3* expression has statistical differences in normal and ccRCC tissues, we examined *SNHG3* expression in HK-2 and 786-O cells. qPCR results showed that compared to HK-2 cells, *SNHG3* expression was elevated in 786-O cells ($P<0.05$; *Figure 6A*). This result was also confirmed on renal cancer specimens from ccRCC patients ($P<0.01$; *Figure 6B*). In order to learn more about *SNHG3*'s biological role in ccRCC, si-*SNHG3* was

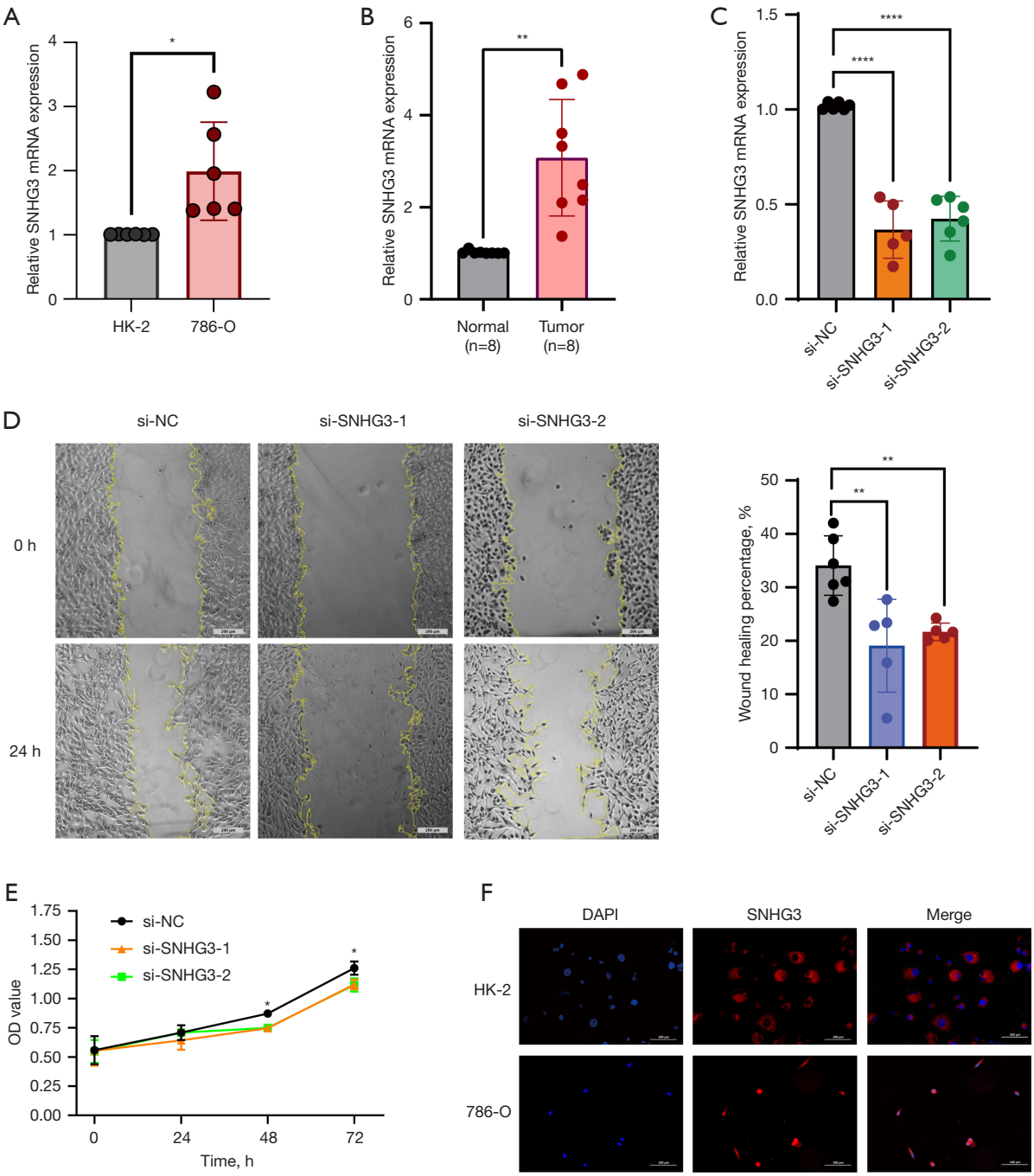

Figure 6 Effects of *SNHG3* on expression, proliferation, and migration of ccRCC cells. (A) Expression levels of *SNHG3* in ccRCC cell lines (n=6). (B) Expression levels of *SNHG3* between normal and tumor samples of ccRCC patients (n=8). (C) The knockdown efficiency of *SNHG3* in 786-O cells was verified by quantitative reverse transcription-polymerase chain reaction. (D) Wound healing assay was used to detect the effect of *SNHG3* on the migration function of tumor cells (n≥5). The migration of cells was observed and recorded by light microscopy and photography, and relative migration rate was calculated by normalizing the distance of the blank area at 0 h. (E) MTT was used to detect the effect of *SNHG3* on the proliferation function of tumor cells (n≥3). (F) Fluorescence in situ hybridization detected the distribution of *SNHG3* in the nucleus of HK-2 and 786-O cells (n=3). *, P<0.05; **, P<0.01; ****, P<0.0001. ccRCC, clear cell renal cell carcinoma; MTT, methylthiazolyldiphenyl-tetrazolium bromide; OD, optical density.

transfected into 786-O cells, and transfection efficiency was assessed (P<0.001; *Figure 6C*). The findings of the wound healing experiment demonstrated that the knockdown of *SNHG3* decreased the ability of tumor cells to migrate (P<0.01; *Figure 6D*). According to MTT findings, tumor cells' ability to proliferate was decreased when *SNHG3* was knocked down (P<0.05; *Figure 6E*). According to the FISH findings, *SNHG3* was present in the cell nuclei of HK-2 and 786-O (*Figure 6F*).

Discussion

In recent years, RCC morbidity and mortality rates have been showing a continuously increasing trend, becoming the seventh most common cancer in the United States (6). Current evidence suggests that ccRCC is the most important factor contributing to death of RCC patients (24). Although surgery is the main treatment for metastatic or non-metastatic ccRCC, there is still a risk of postoperative recurrence. Unfortunately, chemotherapy and radiotherapy exhibit limited efficacy (25).

CcRCC is characterized as a metabolic disease with significant alterations in energy metabolism (26,27). There is a distinct partitioning of metabolic flux through glycolysis, as evidenced in recent studies (28-30). Additionally, studies have shown that various pathogenic mechanisms such as mitochondrial dysfunction, lipid metabolism, and angiogenesis pathogenesis are involved in ccRCC (31-34). Emerging evidence further indicates that the activation of certain metabolic pathways plays a role in modulating angiogenesis and inflammatory signaling, which can contribute to both the onset and progression of ccRCC and potentially lead to drug resistance (35-37). This complexity in pathogenesis presents significant challenges for treatment.

In recent years, with significant progress achieved in science and technology, more biomarkers, including lncRNAs, have been used for the diagnosis and prognosis of malignancies (38-40). LncRNAs can modulate genes at epigenetic, transcriptional, and post-transcriptional levels and regulate the occurrence and outcome of the disease (5,41). Increasing evidence has demonstrated that upregulated *SNHG3* expression links to poor prognosis in various tumors, including ccRCC (42,43). Interestingly, *SNHG3* can promote the proliferation and metastasis of breast cancer cells by inhibiting mitochondrial oxidative phosphorylation and increasing glycolysis level. This suggests the therapeutic potential of *SNHG3* targeting the tumor microenvironment (TME), but whether *SNHG3* also has a similar effect in ccRCC remains unclear (44). Moreover, as ccRCC is one of the most immunologically invasive tumors associated with immune cell infiltration, much literature highlights the potential of immunotherapy, which has garnered significant interest (45-48). Jiang *et al.* found that *SNHG3* could regulate immune cell infiltration and further regulate ccRCC progression by regulating the downstream target genes (49). These findings lead us to associate *SNHG3* with the possibility of regulating immunity in ccRCC, and we speculate that *SNHG3* regulates ccRCC by regulating immunity.

By performing bioinformatics analysis and experimental validation, we found that *SNHG3* could regulate the proliferation and migration functions of ccRCC, which implies that *SNHG3* has the ability to act as a biomarker. In addition, many immune cells, including follicular helper T cells and Tregs were closely related to *SNHG3* with different degrees of infiltration in *SNHG3* high and low expression groups of ccRCC. Subsequently, we conducted survival analyses and found elevated levels of M0 macrophages, Tregs, and follicular helper T cells led to a worse prognosis of ccRCC patients. Subsequently, the relationship between *SNHG3* and various immune checkpoints was explored. Ghini *et al.* showed that inhibition of immune checkpoints enhanced immune escape in Non-small cell lung cancers (50). We also explored the feasibility of immunotherapy and drug sensitivity of *SNHG3*. Our study shares both similarities and distinctions with the work of Xu *et al.* Both studies demonstrated that *SNHG3* regulates the proliferation and metastatic behavior of ccRCC. Xu *et al.* concentrated on identifying a competing endogenous RNA (ceRNA) regulatory axis, which includes *SNHG3*, to explore potential therapeutic targets for ccRCC. Our study reveals an association between *SNHG3* and immune cell infiltration in ccRCC, suggesting a regulatory link between *SNHG3* and the immune microenvironment. This finding highlights the potential of *SNHG3* as a therapeutic target for ccRCC from an immunological perspective (11).

The TME comprises tumor cells and surrounding non-tumor components. In addition to immune cells, TME also includes non-immune cells such as fibroblasts, adipocytes and physical components, which together constitute a dynamically changing environment for the development of tumor cells (51). Research has shown that T cells, especially CD8 T cells, make up a large part of the ccRCC immune microenvironment (52). CD4 T cells that consist of different cell subsets like helper T 1 (TH1) cells, helper T 2 (TH2) cells, helper T 17 (TH17) cells, Tregs, and follicular helper

T cells are also present in the TME. Depending on the physical and chemical properties of the environment, different states of CD4 T cells themselves can have two distinct effects on tumor promotion or inhibition (53). Tregs play a negative regulatory role in immunity and maintain immune homeostasis (53). The expression of various molecules can regulate immune activity within the TME of ccRCC (54-56). The study by Fu *et al.* has demonstrated that Tregs stimulated by interleukin-23 (IL-23) could enhance immunosuppression (57). Consistent with the literature, we found that high level of infiltration of Treg cells was linked to poor outcomes in ccRCC patients. In contrast to Tregs, CD8 T cells are involved in anti-tumor immune responses and may improve patient prognosis. Their infiltration acts as a suppressor of some tumors, including ccRCC. In TME, a reduction in T-reg cell numbers leads to an increase in CD8 T cells, helping to slow tumor growth (58). However, CD8 T cell infiltration showed no such trend in our study. It is well established that M1 and M2 macrophages are differentiated from M0 macrophages. Generally, macrophages are associated with poor prognosis, but strong tumor infiltration by $CD14^{+}CD40^{+}$ macrophages is associated with a good prognosis (59). Interestingly, according to our findings, high M0 infiltration led to poor prognosis in ccRCC patients, unlike M1 and M2 macrophages. The above results suggested that immune cell subpopulations might have different prognostic values depending on their spatial distribution within the tumor. It is important to note that using different algorithms for immune cell profiling may contribute to variable results, highlighting the need for further experimental validation in future studies.

lncRNAs can regulate tumor cellular activities in different ways. It has been shown that lncRNAs can regulate tumor development by recruiting DNA methyltransferases (60,61). Huili *et al.* discovered that some lncRNAs regulate the cuproptosis process in ccRCC (62). Since most lncRNAs regulate tumors by mediating downstream signaling molecules, it is necessary to further study the mediating effect of *SNHG3* on downstream signaling to affect the progression of ccRCC. Liu *et al.* confirmed that knockdown of *COL18A1-AS1/miR-1286*/KLF12 axis regulated lipid browning further repressing ccRCC progression, which again illustrated the diverse regulatory pathways of lncRNA *SNHG3* (63). In addition, the regulation of ccRCC by lncRNA may be related to biological functions such as glycolysis and the maintenance of genomic stability (64,65). It has been shown that the highest enrichment of glycolytic intermediates occurs in primary ccRCC (66), suggesting that regulation of ccRCC through glycolytic metabolism is likely one of the key pathways of lncRNA action. However, further experiments are needed to confirm whether *SNHG3* has similar functions in ccRCC.

The study still has limitations. Firstly, we did not experimentally illustrate the relevance and possible regulatory role of *SNHG3* on immune cell infiltration in ccRCC. By reviewing the literature, we found that most of the results on *SNHG3*'s relationship with immune cell infiltration in the TME of ccRCC or other cancers are largely based on existing database analyses. Secondly, we did not conduct *in vivo* experiments to examine the role of *SNHG3* in ccRCC regulation. We could refer to the findings of Chong Zhang and colleagues, who reported that knockdown of *SNHG3* inhibits ccRCC cell growth and metastasis *in vivo* (43). Thirdly, the specific mechanisms by which *SNHG3* regulates ccRCC remain unclear, and further research is needed to understand its downstream regulatory network and its effect on immune cells. These limitations should be addressed in future studies.

Conclusions

In brief, *SNHG3* promotes the proliferation and migration of ccRCC cells, suggesting that *SNHG3* could be a potential marker for predicting prognosis of ccRCC. Additionally, we discovered that *SNHG3*, correlated to immune cell infiltration, is a potential regulatory and therapeutic target that may create new possibilities for the clinical precision immunotherapy of ccRCC.

Acknowledgments

The authors are grateful to the First Affiliated Hospital of Guangxi Medical University for their support of the present study.

Footnote

Reporting Checklist: The authors have completed the MDAR reporting checklist. Available at https://tcr.amegroups.com/article/view/10.21037/tcr-24-1509/rc

Data Sharing Statement: Available at https://tcr.amegroups.com/article/view/10.21037/tcr-24-1509/dss

Peer Review File: Available at https://tcr.amegroups.com/

article/view/10.21037/tcr-24-1509/prf

Funding: This study was supported by the National Natural Science Foundation of China (No. 81860142).

Conflicts of Interest: All authors have completed the ICMJE uniform disclosure form (available at https://tcr.amegroups.com/article/view/10.21037/tcr-24-1509/coif). The authors have no conflicts of interest to declare.

Ethical Statement: The authors are accountable for all aspects of the work in ensuring that questions related to the accuracy or integrity of any part of the work are appropriately investigated and resolved. The study was conducted in accordance with the Declaration of Helsinki (as revised in 2013). The study was approved by the Ethics Review Committee of the First Affiliated Hospital of Guangxi Medical University (approval No. 2023-E302-01) and informed consent was taken from all individual participants.

References

1. Siegel RL, Giaquinto AN, Jemal A. Cancer statistics, 2024. CA Cancer J Clin 2024;74:12-49.
2. Linehan WM. Genetic basis of kidney cancer: role of genomics for the development of disease-based therapeutics. Genome Res 2012;22:2089-100.
3. Hsieh JJ, Purdue MP, Signoretti S, et al. Renal cell carcinoma. Nat Rev Dis Primers 2017;3:17009.
4. Wolff I, May M, Hoschke B, et al. Do we need new high-risk criteria for surgically treated renal cancer patients to improve the outcome of future clinical trials in the adjuvant setting? Results of a comprehensive analysis based on the multicenter CORONA database. Eur J Surg Oncol 2016;42:744-50.
5. Zhou Y, Zhang Z, Wo M, et al. The long non-coding RNA NNT-AS1 promotes clear cell renal cell carcinoma progression via regulation of the miR-137/ Y-box binding protein 1 axis. Bioengineered 2021;12:8994-9005.
6. Rysz J, Konecki T, Franczyk B, et al. The Role of Long Noncoding RNA (lncRNAs) Biomarkers in Renal Cell Carcinoma. Int J Mol Sci 2022;24:643.
7. Peng Y, Huang X, Wang H. Serum lncRNA LINC01535 as Biomarker of Diagnosis, Prognosis, and Disease Progression in Breast Cancer. Clin Breast Cancer 2023;23:620-7.
8. Chang A, Wang P, Ren J. LINC00963 May Be Associated with a Poor Prognosis in Patients with Cervical Cancer. Med Sci Monit 2022;28:e935070.
9. Peng L, Chen Y, Ou Q, et al. LncRNA MIAT correlates with immune infiltrates and drug reactions in hepatocellular carcinoma. Int Immunopharmacol 2020;89:107071.
10. Zhang F, Lu J, Yang J, et al. SNHG3 regulates NEIL3 via transcription factor E2F1 to mediate malignant proliferation of hepatocellular carcinoma. Immunogenetics 2023;75:39-51.
11. Xu Z, Ye J, Bao P, et al. Long non-coding RNA SNHG3 promotes the progression of clear cell renal cell carcinoma via regulating BIRC5 expression. Transl Cancer Res 2021;10:4502-13.
12. Huang L, Li Y, Wang P, et al. Integrated analysis of immune- and apoptosis-related lncRNA-miRNA-mRNA regulatory network in children with Henoch Schönlein purpura nephritis. Transl Pediatr 2022;11:1682-96.
13. Wang X, Wang J, Lyu L, et al. Oncogenic role and potential regulatory mechanism of topoisomerase IIα in a pan-cancer analysis. Sci Rep 2022;12:11161.
14. Ritchie ME, Phipson B, Wu D, et al. limma powers differential expression analyses for RNA-sequencing and microarray studies. Nucleic Acids Res 2015;43:e47.
15. Therneau TM, Grambsch PM. The Cox Model. In: Therneau TM, Grambsch PM, eds. Modeling Survival Data: Extending the Cox Model. Statistics for Biology and Health. Springer; 2000:39-77.
16. Yu G, Wang LG, Han Y, et al. clusterProfiler: an R package for comparing biological themes among gene clusters. OMICS 2012;16:284-7.
17. Yoshihara K, Shahmoradgoli M, Martínez E, et al. Inferring tumour purity and stromal and immune cell admixture from expression data. Nat Commun 2013;4:2612.
18. Newman AM, Liu CL, Green MR, et al. Robust enumeration of cell subsets from tissue expression profiles. Nat Methods 2015;12:453-7.

19. Li T, Fu J, Zeng Z, et al. TIMER2.0 for analysis of tumor-infiltrating immune cells. Nucleic Acids Res 2020;48:W509-14.
20. Charoentong P, Finotello F, Angelova M, et al. Pan-cancer Immunogenomic Analyses Reveal Genotype-Immunophenotype Relationships and Predictors of Response to Checkpoint Blockade. Cell Rep 2017;18:248-62.
21. Jiang P, Lee W, Li X, et al. Genome-Scale Signatures of Gene Interaction from Compound Screens Predict Clinical Efficacy of Targeted Cancer Therapies. Cell Syst 2018;6:343-354.e5.
22. Geeleher P, Cox N, Huang RS. pRRophetic: an R package for prediction of clinical chemotherapeutic response from tumor gene expression levels. PLoS One 2014;9:e107468.
23. von Roemeling CA, Radisky DC, Marlow LA, et al. Neuronal pentraxin 2 supports clear cell renal cell carcinoma by activating the AMPA-selective glutamate receptor-4. Cancer Res 2014;74:4796-810.
24. Capitanio U, Bensalah K, Bex A, et al. Epidemiology of Renal Cell Carcinoma. Eur Urol 2019;75:74-84.
25. Rini BI, Campbell SC, Escudier B. Renal cell carcinoma. Lancet 2009;373:1119-32.
26. di Meo NA, Lasorsa F, Rutigliano M, et al. The dark side of lipid metabolism in prostate and renal carcinoma: novel insights into molecular diagnostic and biomarker discovery. Expert Rev Mol Diagn 2023;23:297-313.
27. di Meo NA, Lasorsa F, Rutigliano M, et al. Renal Cell Carcinoma as a Metabolic Disease: An Update on Main Pathways, Potential Biomarkers, and Therapeutic Targets. Int J Mol Sci 2022;23:14360.
28. Bianchi C, Meregalli C, Bombelli S, et al. The glucose and lipid metabolism reprogramming is grade-dependent in clear cell renal cell carcinoma primary cultures and is targetable to modulate cell viability and proliferation. Oncotarget 2017;8:113502-15.
29. Ragone R, Sallustio F, Piccinonna S, et al. Renal Cell Carcinoma: A Study through NMR-Based Metabolomics Combined with Transcriptomics. Diseases 2016;4:7.
30. Lucarelli G, Galleggiante V, Rutigliano M, et al. Metabolomic profile of glycolysis and the pentose phosphate pathway identifies the central role of glucose-6-phosphate dehydrogenase in clear cell-renal cell carcinoma. Oncotarget 2015;6:13371-86.
31. Lucarelli G, Rutigliano M, Sallustio F, et al. Integrated multi-omics characterization reveals a distinctive metabolic signature and the role of NDUFA4L2 in promoting angiogenesis, chemoresistance, and mitochondrial dysfunction in clear cell renal cell carcinoma. Aging (Albany NY) 2018;10:3957-85.
32. Bombelli S, Torsello B, De Marco S, et al. 36-kDa Annexin A3 Isoform Negatively Modulates Lipid Storage in Clear Cell Renal Cell Carcinoma Cells. Am J Pathol 2020;190:2317-26.
33. Lucarelli G, Rutigliano M, Loizzo D, et al. MUC1 Tissue Expression and Its Soluble Form CA15-3 Identify a Clear Cell Renal Cell Carcinoma with Distinct Metabolic Profile and Poor Clinical Outcome. Int J Mol Sci 2022;23:13968.
34. Milella M, Rutigliano M, Lasorsa F, et al. The Role of MUC1 in Renal Cell Carcinoma. Biomolecules 2024;14:315.
35. Netti GS, Lucarelli G, Spadaccino F, et al. PTX3 modulates the immunoflogosis in tumor microenvironment and is a prognostic factor for patients with clear cell renal cell carcinoma. Aging (Albany NY) 2020;12:7585-602.
36. Lucarelli G, Loizzo D, Franzin R, et al. Metabolomic insights into pathophysiological mechanisms and biomarker discovery in clear cell renal cell carcinoma. Expert Rev Mol Diagn 2019;19:397-407.
37. De Marco S, Torsello B, Minutiello E, et al. The cross-talk between Abl2 tyrosine kinase and TGFβ1 signalling modulates the invasion of clear cell Renal Cell Carcinoma cells. FEBS Lett 2023;597:1098-113.
38. Lasorsa F, Rutigliano M, Milella M, et al. Cancer Stem Cells in Renal Cell Carcinoma: Origins and Biomarkers. Int J Mol Sci 2023;24:13179.
39. Feng W, He Z, Shi L, et al. Significance of CD80 as a Prognostic and Immunotherapeutic Biomarker in Lung Adenocarcinoma. Biochem Genet 2023;61:1937-66.
40. Ren Z, He Y, Yang Q, et al. A Comprehensive Analysis of the Glutathione Peroxidase 8 (GPX8) in Human Cancer. Front Oncol 2022;12:812811.
41. Zhao Z, Sun W, Guo Z, et al. Mechanisms of lncRNA/microRNA interactions in angiogenesis. Life Sci 2020;254:116900.
42. He WW, Ma HT, Guo X, et al. lncRNA SNHG3 accelerates the proliferation and invasion of non-small cell lung cancer by downregulating miR-340-5p. J Biol Regul Homeost Agents 2020;34:2017-27.
43. Zhang C, Qu Y, Xiao H, et al. LncRNA SNHG3 promotes clear cell renal cell carcinoma proliferation and migration by upregulating TOP2A. Exp Cell Res 2019;384:111595.
44. Li Y, Zhao Z, Liu W, et al. SNHG3 Functions as miRNA Sponge to Promote Breast Cancer Cells Growth Through the Metabolic Reprogramming. Appl Biochem Biotechnol 2020;191:1084-99.

45. Vuong L, Kotecha RR, Voss MH, et al. Tumor Microenvironment Dynamics in Clear-Cell Renal Cell Carcinoma. Cancer Discov 2019;9:1349-57.
46. Tamma R, Rutigliano M, Lucarelli G, et al. Microvascular density, macrophages, and mast cells in human clear cell renal carcinoma with and without bevacizumab treatment. Urol Oncol 2019;37:355.e11-9.
47. Gigante M, Pontrelli P, Herr W, et al. miR-29b and miR-198 overexpression in CD8+ T cells of renal cell carcinoma patients down-modulates JAK3 and MCL-1 leading to immune dysfunction. J Transl Med 2016;14:84.
48. Ged Y, Markowski MC, Singla N, et al. The shifting treatment paradigm of metastatic renal cell carcinoma. Nat Rev Urol 2022;19:631-2.
49. Jiang Y, Han D, Zhao Y, et al. Multi-Omics Analysis of the Prognosis and Biological Function for TRPV Channel Family in Clear Cell Renal Cell Carcinoma. Front Immunol 2022;13:872170.
50. Ghini V, Laera L, Fantechi B, et al. Metabolomics to Assess Response to Immune Checkpoint Inhibitors in Patients with Non-Small-Cell Lung Cancer. Cancers (Basel) 2020;12:3574.
51. Lai Y, Tang F, Huang Y, et al. The tumour microenvironment and metabolism in renal cell carcinoma targeted or immune therapy. J Cell Physiol 2021;236:1616-27.
52. Monjaras-Avila CU, Lorenzo-Leal AC, Luque-Badillo AC, et al. The Tumor Immune Microenvironment in Clear Cell Renal Cell Carcinoma. Int J Mol Sci 2023;24:7946.
53. Siska PJ, Rathmell JC. T cell metabolic fitness in antitumor immunity. Trends Immunol 2015;36:257-64.
54. Lasorsa F, Rutigliano M, Milella M, et al. Complement System and the Kidney: Its Role in Renal Diseases, Kidney Transplantation and Renal Cell Carcinoma. Int J Mol Sci 2023;24:16515.
55. Lasorsa F, di Meo NA, Rutigliano M, et al. Immune Checkpoint Inhibitors in Renal Cell Carcinoma: Molecular Basis and Rationale for Their Use in Clinical Practice. Biomedicines 2023;11:1071.
56. Lucarelli G, Netti GS, Rutigliano M, et al. MUC1 Expression Affects the Immunoflogosis in Renal Cell Carcinoma Microenvironment through Complement System Activation and Immune Infiltrate Modulation. Int J Mol Sci 2023;24:4814.
57. Fu Q, Xu L, Wang Y, et al. Tumor-associated Macrophage-derived Interleukin-23 Interlinks Kidney Cancer Glutamine Addiction with Immune Evasion. Eur Urol 2019;75:752-63.
58. Lasorsa F, Rutigliano M, Milella M, et al. Cellular and Molecular Players in the Tumor Microenvironment of Renal Cell Carcinoma. J Clin Med 2023;12:3888.
59. Krenciute G, Prinzing BL, Yi Z, et al. Transgenic Expression of IL15 Improves Antiglioma Activity of IL13Rα2-CAR T Cells but Results in Antigen Loss Variants. Cancer Immunol Res 2017;5:571-81.
60. Huang W, Li H, Yu Q, et al. LncRNA-mediated DNA methylation: an emerging mechanism in cancer and beyond. J Exp Clin Cancer Res 2022;41:100.
61. Su SC, Yeh CM, Lin CW, et al. A novel melatonin-regulated lncRNA suppresses TPA-induced oral cancer cell motility through replenishing PRUNE2 expression. J Pineal Res 2021;71:e12760.
62. Huili Y, Nie S, Zhang L, et al. Cuproptosis-related lncRNA: Prediction of prognosis and subtype determination in clear cell renal cell carcinoma. Front Genet 2022;13:958547.
63. Liu Y, Wang J, Shou Y, et al. Restoring the epigenetically silenced lncRNA COL18A1-AS1 represses ccRCC progression by lipid browning via miR-1286/KLF12 axis. Cell Death Dis 2022;13:578.
64. Li T, Tong H, Zhu J, et al. Identification of a Three-Glycolysis-Related lncRNA Signature Correlated With Prognosis and Metastasis in Clear Cell Renal Cell Carcinoma. Front Med (Lausanne) 2021;8:777507.
65. Yang H, Xiong X, Li H. Development and Interpretation of a Genomic Instability Derived lncRNAs Based Risk Signature as a Predictor of Prognosis for Clear Cell Renal Cell Carcinoma Patients. Front Oncol 2021;11:678253.
66. Courtney KD, Bezwada D, Mashimo T, et al. Isotope Tracing of Human Clear Cell Renal Cell Carcinomas Demonstrates Suppressed Glucose Oxidation In Vivo. Cell Metab 2018;28:793-800.e2.

Cite this article as: Li C, Hu P, Fan C, Mi H. The prognostic and immune significance of *SNHG3* in clear cell renal cell carcinoma. Transl Cancer Res 2025;14(2):1008-1023. doi: 10.21037/tcr-24-1509

